On Dry and Wet Corrosion of Iron

M. I. ISMAIL* and N. SATO

Corroion Research Group, Faculty of Engineering, Hokkaido University, Sapporo, Japan

(Received September, 30, 1974)

Abstract

Metallographic and polarographic techniques were used to study the rule played by metal substrate metallurgical conditions on corrosion of pure iron. Different heat treatment cycles were employed, viz: 1 hour at 600–900°C, 10^{-3} Torr, rapidly cooled (WQ), or slowly furnace cooled (FC), or rapidly heated specimens in air (30 sec, 1000 C, air cooled); and the effect of heat treatment cycling. It was found that the oxide film formed in air has random orientation while the one formed in vacuum is oriented. ostatically corrosion was determined by measuring the anodic current under potenti- The rate ofcontrolled dissolution in 0.1 NH_2SO_4 at 20 C. The anodic current decay during polarization, the amount of dissolved metal and surface morphology were used to clarifythe effect of heat treatment in corrosion of iron.

1. Introduction

Several investigators heve studied the different parameters affecting corrosion of iron[1–12]. Usually it has been investigated from stand point of electrochemistry[13–15] and rarely from the stand point of metal substrate[16,17]. However, metallographic study can provide important possible answers to the problems of active dissolution or corrosion of iron. Metal substrate grain size and internal stresses are controlled by the different heat treatment cycles (temperature, time, and rate of cooling). The aim of this work was to clarify the interrelationship between metal substrate and surface behaviour of pure iron.

Experimental

Plates of pure iron (99.9%) have the following analysis in wt. per cent: Ni, 0.040; Cr, 0.001; Si, 0.008 S, 0.002; Mn, 0.0005; Mo, 0.001; C, 0.0035; and Cu, 0.002. Rectangular specimens were machined from a 1 mm thick rolled plate. Different heat treatment cycles were conducted to the mechanically polished and ultrasonically cleaned specimens in the normal way. The heat treatment cycles were as follows: 600–900°C for 1 hour at 10^{-3} Torr with a very slow rate of cooling (0.001°C/Sec), FC, or with a very high rate of cooling (100°C/Sec), that is, ice-colled water, WQ. In both cases pressure inside the silica tube was kept 10^{-3} Torr, during heat treatment cycles. Short heating cycles (30 Sec at 1000°C, with air cooling at atmospheric pressure) were also applied. Specimens used for polarization were once more mechanically polished, ultrasonically cleaned, washed and dried. The electrolyte solution was 0.1 N H_2SO_4. The electrochemical cell and the experimental technique have been described previously[18]. Metallographic examination of surfaces was

* Permanent Addres: Faculty of Engineerig, Alexandria University, Alexandria, Egypt.

used to follow surface behaviour after differrent processes, such as heat treatment, polarization, chemical etching, or severe chemical attack by HF/H_2O_2[19].

Results

Different heat-treatment cycles were applied to mechanically polished pure iron. The current decay values, during polarization of these specimens in 0.1 N H_2SO_4 at 1200 mv and 20°C, are shown in Figure 1. Mostly the current density (cd) decreased with time, otherwise active dissolution occurred and the cd increases or remains constant. But when the applied potential is in the active range (600 mV) then most of the specimens dissolved rapidly. In a very few cases, the cd decayed to lower values as indicated by Figure 2. At the initial stages of electrolysis (1–10 sec) the cd decreased with the increase in temperature, at which the metal was initially heat-treated (Figure 3). Specimens heated for only 30 sec at 1000°C and then air cooled have low cd, after electrolysis for 100 sec, even if an active potential of 600 mV is used as shown in Figure 4. Figure 5 shows that at passive potential (1200 mV) during the initial stages the relative increase in current (measured as the current after 1 or 10 sec from the start of electrolysis to the current after 10 or 100 sec respectively) decayed with time. At an active potential (600 mV) there was always an active dissolution and current decay was negligible for both WQ and FC specimens but higher current decay ratio is noted for air cooled specimens (Fig. 6). It is worth mentioning that when the same heat treatment cycle was repeated, the final cycle gave a more corrosion resistant surface, i. e. a lower cd. Atmic absorption spectrophotometric analysis of the solution after polaization for 10 min at 1200 mV (Fig. 7) indicated that the amount of dissolved iron (Fe^{2+}) decreased with heat treatment temperature for the WQ

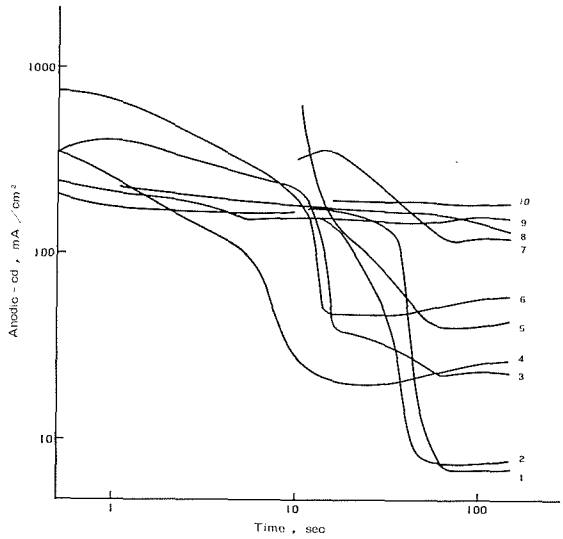

Fig. 1 Current decay curves of heat treated pure iron in 0.1 N H_2SO_4 at 20°C and 1200 mV, sce. Heat treatment cycle: Temperature, °C; Time, hour or sec; Cooling rate (rapid, WQ; slow, FC; or air cooling, AC) 1, 900, 1h, WQ; 2, 800, 1h, FC; 3, 950, 1h, FC: 2 cycles; 4, 1000, 30 Sec, AC; 5, 600, 1h, WQ; 6, as received; 7, 800, 1h, WQ+800, 1h, FC; 8, 950, 1h, FC; 9, 800, 1h, FC: 2 cycles; and 10,800, 1h, WQ

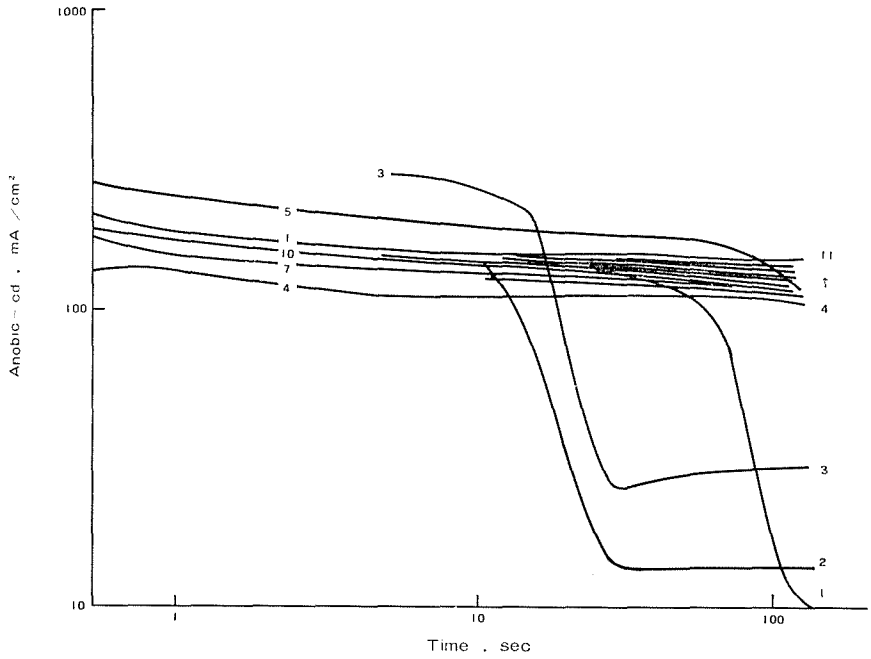

Fig. 2 Current density-time curves of heat treated pure iron in 0.1 N H_2SO_4 at 20°C and 600 mV, sec. Heat treatment cycle: Temp., C; Time: Cooling rate. 1, 950, 1h, FC: 2 cycles; 2, 1000. 30 sec, AC; 3, as received; 4, 800, 1h, FC: 2 cycles; 5, 800, 1h, WQ+800, 1h, FC; 6, 950, 1h, FC; 7, 800, 1h, FC; 8, 900, 1h, WQ; 9, 600, 1h, WQ+800, 1h, WQ; 10, 800, 1h, WQ; and 11, 600, 1h, WQ

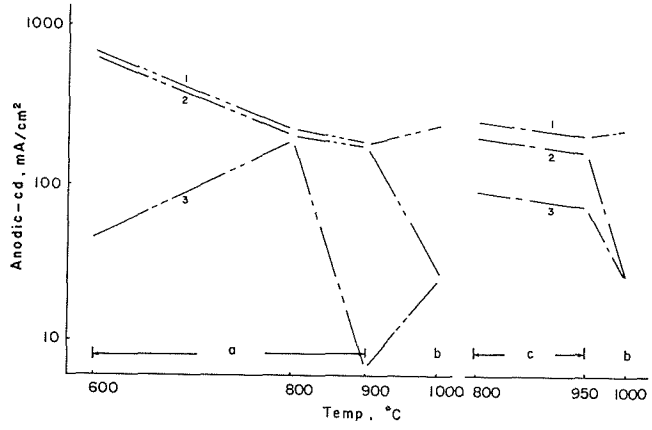

Fig. 3 Current density vs temperature of heat treatment of polarized iron in 0.1 N H_2SO_4 at 20°C and 1200 mV, sce. Heat treatment cycle: Time, cooling rate. a) 1h, WQ; b) 30 sec, AC; and c) 1h, FC. Polarization time: 1, 1 sec; 2, 10 sec; and 3, 100 sec

specimens. FC specimens behave reversely, i.e. the amount of dissolved iron increased with the increase in heat treatment temperature.

Surface Morpholology of Scale formed during Heat Treatment:

Metallographic examination of the thermal oxides formed during heat treatment (Figs. 8 and 9) indicated that at lower temperature (600°C) grain boundaries are thermally etched as they have lower surface level than the grains. At 950°C

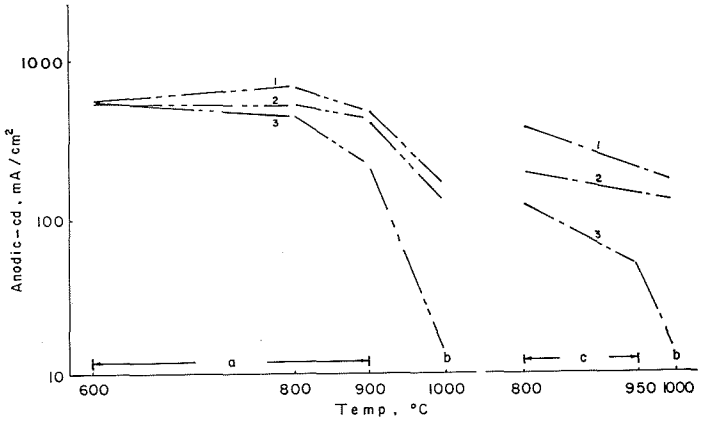

Fig. 4 Current density vs heat treatment temperature of polarized iron in 0.1 N H_2SO_4 at 20°C and 600 mV, sce. Heat treatment cycle: Time, cooling rate. a) 1h, WQ, b) 30 sec, AC; and c) 1h, FC. Polarization time: 1, 1 sec; 2, 10 sec; and 3, 100 sec

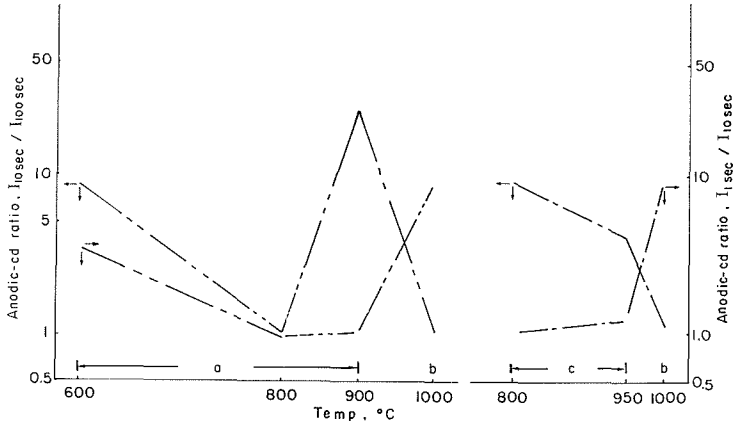

Fig. 5 Current decay ratio (I 1 sec/I 10 sec or I 10 sec/I 100 sec.) vs temperature of heat treatment of polarized iron in 0.1 N H_2SO_4 at 20°C and 1200 mV, sce. Heat treatment cycle: Time, cooling rate. a) 1h, WQ; b) 30 sec, AC; and c) 1h, FC

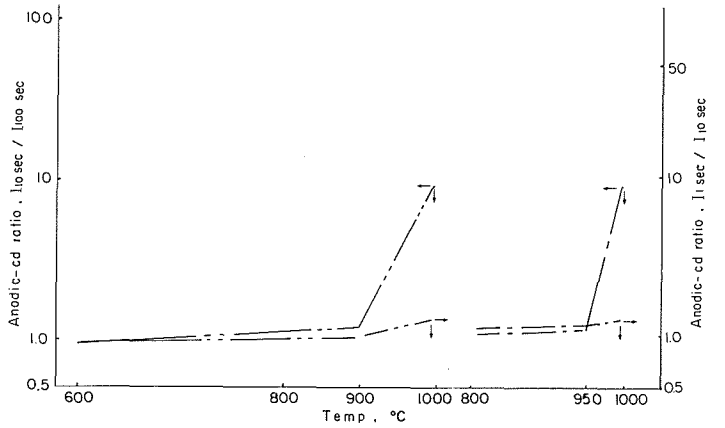

Fig. 6 Current decay ratio vs temperature of heat treatment of polarized iron in 0.1 N H_2SO_4 at 20°C and 600 mV, sce. Heat treament cycle: Time, cooling rate. a) 1h, WQ: b) 30 sec, AC; and c) 1h, FC

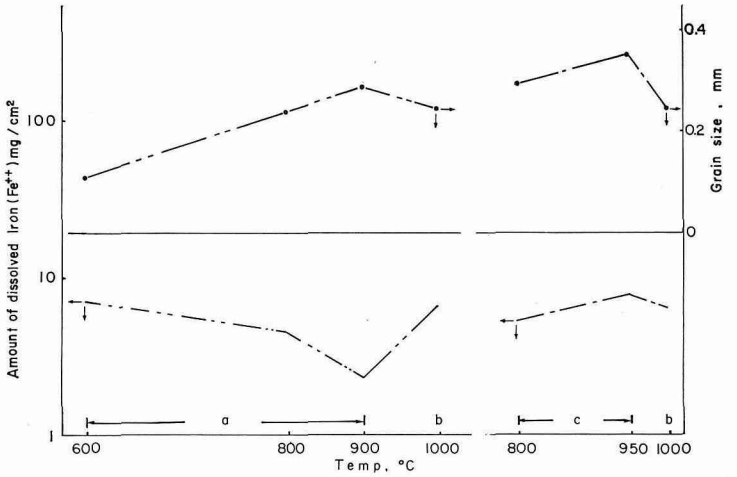

Fig. 7 Amount of dissolved iron (Fe^{++}), substrate grain size and heat treatment temperature relationship of polarized iron in 0.1 N H_2SO_4 at 20°C and 1200 mV. Polarization time 10 min. Heat treatment cycle: Time, cooling rate. a) 1h, WQ; b) 30 sec, AC; and c) 1h, FC

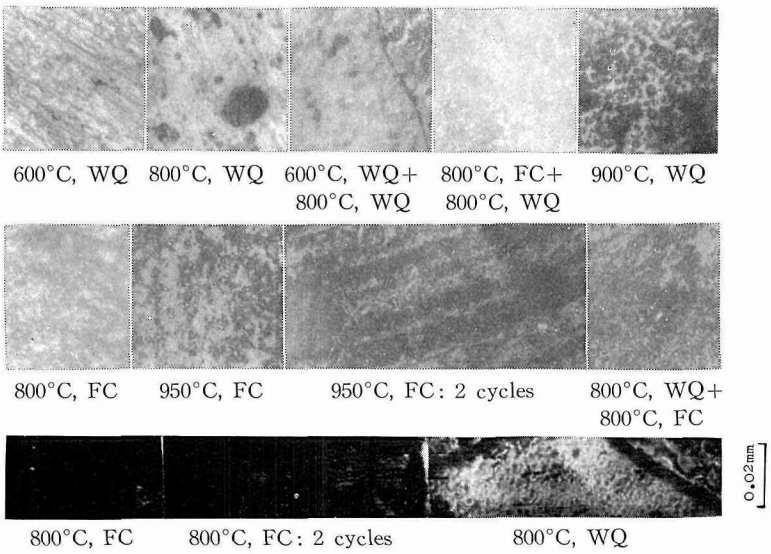

Fig. 8 Photomicrographs of oxide films formed during heat treatment in vaccum (1h 10^{-3} Torr). a) WQ; b) FC; and c) FC and WQ exposed to air for 8 months

numerous pores were observed. At a very slow cooling rates from 800°C a continuous pore-free surface was obtained and the resultant scale has a uniform structucture. On reheating and slow cooling again the previously formed oxides showed larger grain boundaries and also had a uniform, apparently non-porous structure. Rapid rates of cooling from high temperatures (100°C/see; 900°C) resulted in formation of pores or pits. But rapid cooling from lower temperature (600°C, 1000°C/sec) gave no indication of pores but only differential oxidation or rusting. On slow cooling from 800°C (0.01°C/sec) surface was covered with oxide islands which on reheating and slow cooling again resulted in a uniform more

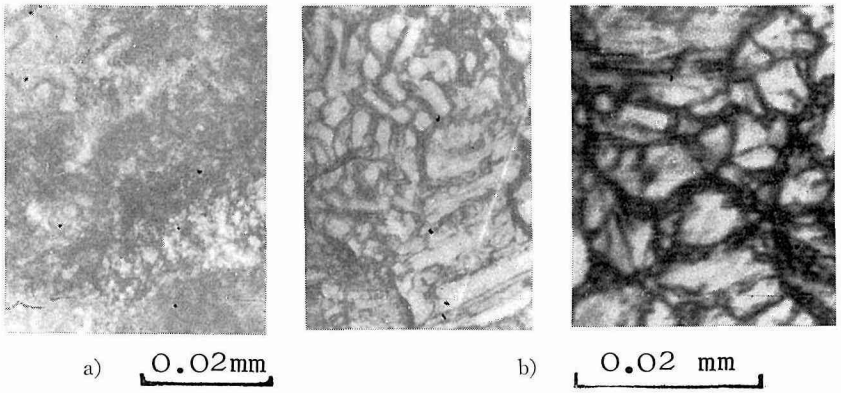

Fig. 9 Photomicrographs of oxides formed on iron during short period of heating in air. (30 sec, 1000°C, AC). a) 1 cycle, and b) 4 cycles

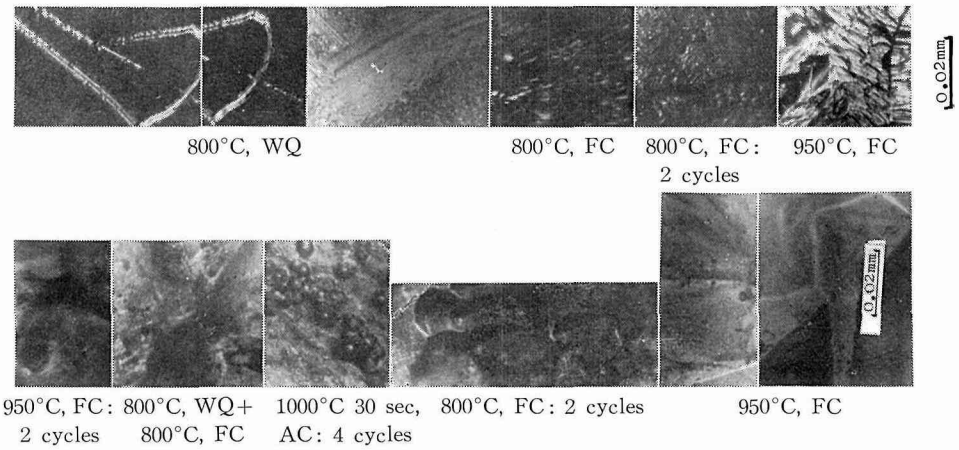

Fig. 10 Photomicrographs of specimen after polarization (10 min) in 0.1 N H_2SO_4 at 20°C and 1200 mV, sce

refined film. Large stains or pores were frequently seen. Rapid cooling from 800°C (100°C/sec) resulted in rust type oxides which on further heating to 800°C and slow cooling resulted in the formation of some pores.

Rapid heating of iron in air (30 see at 1000°C) resulted in a seale full of pores but sometimes oxide covered a continuous area of no pores. Short time heating at high temperatures then air cooling as mentioned above, repeating this cxcle several times produced a thermally etched undulating surface of wide grain boundaries (Fig. 9). Oxides formed on heat treated iron (8 month exposure to ambient conditions is the presence of normal indoor atmospheric impurities in Sapporo) indicated corrosion by darkening, followed by rusting or formation of non-adhesive corrosion products (Fig. 8).

Metal Substrate Behaviour and Heat Treatment:

Metal substrate grain size increased with heat treatment temperature. It is worth mentioning that at higher temperatures, grain refinement occurred when the heat treatment cycle was repeated more than once. Chemical etching (1% Nital for 4 h) is also selective to heat treatment. Selective differential attack even in the same grain was common to high temperature heat treated specimens. Stepwise dissolution was also common in FC specimens during chemical attack (Fig. 10).

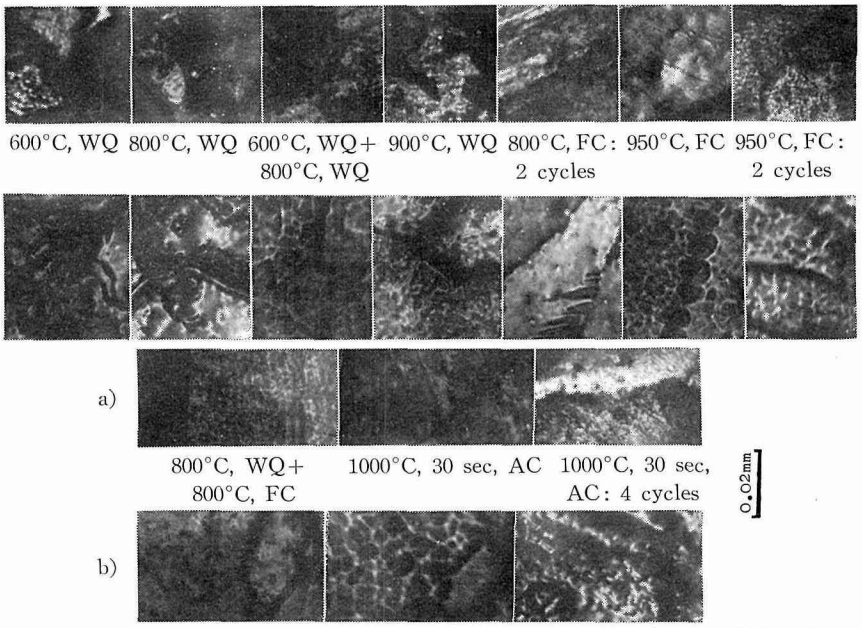

Fig. 11 Photomicrographs of specimens after chemical attack. a) 1% Nital for 4 hours at 20 C; b) HF/H_2O_2 (80% H_2O_2 (30% conc); 15% H_2O; and 5% HF (48% conc)) for 20 sec at 20°C

These bands are more corrosion resistant than the uniform portions of the surface even when treated with aggressive chemical agent (HF/H_2O_2)[19] which attacked the metal. Severe chemical attack by HF/H_2O_2 mixture (15 sec at 20°C) resulted in the formbtion of deep wide pores (Fig. 11). pores are common in grain boundaries and to a less extent in grains but it took sometimes regular ordering, e. g. one raw, twins or three together.

Discussion

A. Dry Corrosion of Iron:

Thermal oxidation of iron leads to the formation of iron oxides which change with time and temperature. Paidassi[20,21] employing a micrographical method found that the individual oxides FeO (Wüstite), Fe_3O_4 and α–Fe_2o_3 all grew parabolically on the iron oxidized in air at 700–1250°C. Also, Fe_3O_4 and α–Fe_2O_3 each grew paradolically on the Wüstite oxidized in air at 600–1000°C. With both the metal and Wüstite as starting matriael, the activation energy for hematite growth was in the region of 45 Kcal/mol. Whether the anions were the faster-diffusing species in the growing α–Fe_2o_3 or the cations, is yet to be settled. Davies et al.[22] reported that hematite grew by anion diffusion. In a more recent observations, however, Holt and Himmel[23] had concludad that iron was the faster moving species. Employng ^{18}O tracare (activated after oxidation by proton irradiation), they found that oxygen was virtually immobile in α–Fe_2O_3 and that the migrating species was iron.

In growing magnetite iron is the mobile species[24]. In the presence of a covering film of α–Fe_2O_3 the vacancy gradient across Fe_3O_4 is independent of external gas pressure[25]. The increase of rate of oxidation by cycling the temperature

of oxidation may be an effect of strain introduced into the scale during thermal cycling[7].

The influence of crystallographic orientation on oxidation rate is due to the variation of work function[26], the structure of a pre-nucleated surface layer[27] or due to lattice mismatch[28] with orientation. Ali and Wood[2] in their study of the oxidation of iron at room temperature indicated that impurities (water vapour, carbon compounds, sulfur compounds and organic substances) in air have little influence on the oxidation rate for the first 20–30 days. A subsequent increase in oxidation rate and the appearance of α–Fe_2O_3 have been related to the catalytic effects of atmospheric impurities since neither of these effects occur in pure dry air[13–15,29–31]. The rapid rise in oxidation rate of iron at room temperature after 60 days is related to metal grain boundary effects[2]. Rhodin[32] concluded that the oxide film on stainless steel contained 30–40% bound water. Hoar[33], in a work on electron spectra of oxide films on pure iron, reported that the binding-energy and intensity differences suggest air- formed oxide film on pure iron is Fe_2O_3, while the anodically produced film on pure iron (in boiling $ca(NO_3)_2$ at-335 to-250 mV sec) is Fe_3O_4 which is formed underneath the Fe_2O_3 air formed film, when this is initially present. Employing Mössbaur spectroscopy[5,34], Fe_2O_3 and Fe_3O_4 have been identified in certain oxide films formed on iron at 450°C. The three iron oxides (Wüstite, Fe_2O_3 and Fe_3O_4) show distinct visual characteristics when crystallized from the melt as a primary phases[35]. The term Wüstite is preferred since the formula FeO never coincides stoichiometrically with the Wüstite phase[36–39]. It is clear from the Fe–O diagram illustrated by Hansen[40] that Fe_2O_3 dissociates at 1457°C into Fe_3O_4 while liquid Fe_3O_4 solidifies congruently to give a solid compound ($FeO \cdot Fe_2O_3$), with spinel structure. The degree of solid solubility of oxygen in both Fe_2O_3 and Fe_3O_4 is very low (nil at 750°C). Wüstite is present as an intermediate phase stable above 560°C. Below this temperature it decomposes eutectsidally under equilibrium conditions (very slow rate of cooling) into Fe_3O_4 and iron. The amount of Fe_3O_4 in the oxide film depends on the rate of cooling[41]. Solid state transformation are responsible for the changes in oxidation rate. The volume decrease associated with change of α–Fe to γ–Fe at 910°C is about 50% (BCC——FCC) this leads to localized loss of scale metal contact. This is in accordance with recent report on adhesion of oxide scale on iron[42]).

Since the carbon content of the used iron (0.0035% wt.) exceeded the solubility limit in the Fe–Fe_3C diagram (0.0025% wt. at room temperature) and thus the tendency to form carbides during slow cooling is possible. Chrome carbide ($Cr_{23}C_6$) is reported to precipitate in the grain boundaries of sensitized iron[43]. Molybdenum is known to decrease susceptibility to sensitization.

Iron surface morphology after heat treatment indicated that FC specimens were more irregular than the WQ ones. This suggests the formation of voids at the oxide-metal interface before separation. The presence of grain boundary voids, as indicated by microphotographs, suggests vacancy movement in the metal as a result of cation movement towards the oxide-metal interface. Once the vacancies is moved towards the grain boundary of metal substrae, it condenses there and form pores. These pores are enlarged in size when specimens were treated with strong chemical agents (HF/H_2O_2)[19] as shown in Figure 11. Thermal oxides thicking at the grain boundaries, as revealed by metallographic examination, supported the above postulation. Recently, it was reported that bulk diffusion characteristics of the iron substrate does not appear to play an important part in

Table 1 Physical properties of iron and its oxides

Material	Thermal expansion coefficient $\times 10^{-6}$	Atomic radius Å	Ionic radius Å	Oxide-metal volume ratio	density g/cm^3
iron	15.3 (0–900°C)	1.26	0.75 (Fe^{2+}) 0.67 (Fe^{3+})	—	
Wüstite (Fe_xO)	12.2 (100–1000°C)	—	—	1.70	5.70
Magnetite (Fe_3O_4)	—	—	—	2.10	5.18
Hematite (Fe_2O_3)	—	—	—	2.14	
Oxygen	—	0.60	1.4 (O^{2-})	—	

the oxidation of iron[1]. According to Noden et al.[44] a compressive stress is developed within the growing oxide layer on austenitic steel. Stresses are generated in the oxide film on cooling from the heat-treatment temperature, with a resultant loss of adhesion from the metal substrate. The separation of scale on cooling is due to differential thermal contraction of the oxide/metal couple[4]. The physical properties of iron and its oxides[1,9] are shown in Table 1.

Fron the previous discussion it is clear that there are several possibilities to explain the variation of surface morphology, such as dislocation movement, volatilization of oxidation products at high temperatures, and surface reaction with environmental gas during heat treatment cycle.

B. Wet Corrosion of Iron :

Because of the electrochemical nature of the corrosion process, it would seem reasonable to use electrochemical measurements to detect susceptibility to intergranular corrosion by the measurement of current density of potentiostatically controlled polarized specimens. A specimen would be considered to be susceptible if the steady-state cds were above a certain critical value. The increase in applied current of a susceptible sample over that of an unsusceptible one, would be due to the increased cd at the grain boundary. The grain boundary area dissolves at a much higher rate than the matrix. After a short time of polarization (e. g. 10 min), the intergranular attack can be observed metallographically. Oxide film on iron is easily reducible, but the current for iron dissolution prevails and masks the current of oxide reduction[45]. Active anions produce pitting and high currents in the passive potential region. Their influence on film breakdown, and therefore on increased metal dissolution, is still a subject of much discussion[46]. Many workers have studied these phenomena upon iron[46–50]. The observed pitting is not crystallographic, but hemi-spherical, with the formation of highly reflecting surfaces. Breakdown sites are usually observed at the grain boundaries where the film is less perfect. In the passive potential region, the current is independent of potential and decreases continuously with time[51,52]. Chemical dissolution (independent of potential and film thickness) accounts for only a very small part of the total dissolution[53]. In the active potential region dissolution is hindered by a decrease in the free electrode area, while in the passive region dissolution depends entirely on the properties of the passivating film[45]. The rate of the anodic process as a function of time[54] due to an increase of the exchange cd for the Fe/Fe^{2+} reaction. This increase occurs despite an enoblement of the reversible potential for this reaction as the Fe^{2+} content of the solution increases[55].

A correlation between thermal and anodic oxide growth behaviour on some metals has been reported recently[56]. The driving force for oxide growth during the thermal oxidation is the temperature. In the anodic growth, the driving force

is the field required to sustain a given value of the ionic cd. The latter is responsible for the conversion of the metal to the corresponding oxide. Recently, Vijh[56] concluded that there exists a relation between the driving force of thermal oxidation (the temperature at which weight change of 1 mg/cm^2–4h was achieved) and that of anodic oxidation (field at a given cd). Higher values of temperature are associated with higher field. It should be mentioned that it is not possible to sustain appreciable anodic oxide growth on all metals, simply because anodization in electrolyte solutions can lead to other simultaneous reactions that occur along with oxide growth. Examples are oxidation of the electrolyte components, oxygen evolution, and anodic dissolution of metals[57,58].

In concentrated sulfuric acid (79%) iron corroded with the formation of a thick layer of corrosion products consisting mainly of iron sulfates[59]. In the active potential range, iron dissolves via two electrochemical stages connected by $(FeOH)_{ads}$[60]. It is demonstrated that the formation of $(FeOH)_{ads}$ layer precedes primary passivity[60]. A reaction scheme[60–64] has been suggested to illustrate the succession of activity, passivity, and transpassivity pehnomena. The corrosion of a metal dissolving stepwise with the formation of low-valency intermediates and M^{n+} ions, as a final corrosion product proceeds by a complex electrochemical—chemical mechanism comprising several steps[65].

Acknowledgement

Financial support granted to one of us (M.I.I.) during the course of this work, by The Japan Society for Promotion of Science (JSPS), is gratefully acknowledged.

References

1) Carpenter, D. L. and Ray, A. C.: Corros. Sci., 13 (1973), p. 493.
2) Ali, S. I. and Wood G. C.: Br. Corros. J., 4 (1969), p. 133.
3) Whittle, D. P.: Corros. Sci., 12 (1972), p. 869.
4) Francis, J. M. and Hodgson, K. E.: Inter. Cong. Met Corros., 4 (1969), p. 1.
5) Simmons, G. W. Kellerman, E. and Leidheiser, H. Jr., Corr. Nace., 29 (1973), p. 227.
6) Channing, D. A. and Graham, M. J.: Corros. Sci., 12 (1972), p. 271.
7) Fleetwood, M. J. and Whittle, J. E.: Br. Corros. J., 5 (1970), p. 131.
8) Hough, R. R. and Rolls, R.: Met. Sci., 5 (1971), p. 206.
9) Caplan, D. and Cohen, M.: Corros. Sci., 6 (1969), p. 321.
10) Caplan, D., Sproul, G. I. and Hussey, R. J.: Corros. Sci., 10 (1970), p. 9.
11) Ali, S. I. and Wood, G. C.: J. Inst. Metals., 97 (1969), p. 6.
12) Caplan, D., Graham, M. J. and Cohen, M.:Corros. Sci., 10 (1970), p. 1.
13) Hancock, P. and Mayne, J. E. O.: J. Chem. Soc., (1958), p. 4167.
14) Davaies, D. E., Evans, U. R. and Agar, J. N.: Proc. R. Soc. (A), 225 (1954), p. 443.
15) Sewell, P. B. Stockbridge, C. D. and Cohen, M. J.: J. Electrochem. Soc., 108 (1961), p. 933.
16) Hisamatsu, Y.: Denki Kagaku, 38 (1970), p. 691.
17) Ohtani, N.: Iron Steel (Japan), 60 (1974), p. 1.
18) Ismail, M. I. and Sato, N.; The role of straining in the electrochemical and mechanical behaviour of pure iron. Submitted for publication.
19) Christ, B. W. and Smith, L. C.: J. Iron Steel Ins. Feb. 1973, p. 155.
20) Paidassi, J.: Acta Met., 6 (1958), p. 219.
21) Paidassi, J.: Acta Met., 6 (1958), p. 184.
22) Davies, M. H., Simnad, M. T. and Birchenall, C. E.: Trans. Aime. J. Metals., 3 (1951), p. 889.
23) Holt, J. B. and Himmel, L.: J. Electrochem. Soc.; 116 (169), p. 1569.

24) Hauffe, K.: Oxidation of Metals., p. 280.; Plenum Press, N. Y. (1965).
25) Boggs, W. E., Kachik, R. H. and Pellissier, G. E.: J. Electrochem. Soc., 112 (1965), p. 539.
26) Uhlig, H. H.: Acta Metall., 4 (1956), p. 541.
27) Ronnquist, A. and Thomas, K.: Br. Corros. J., 1 (1965), p. 47.
28) Lawless, K. R. and Gwathmey, A. T.: Acta Metall., 4 (1956), p. 153.
29) Kruger, J. and Yolken, H. I.: Corrosion, 20 (1964), p. 29 t.
30) Cohen, M. S.: Acta Metall., 8 (1960), p. 356.
31) Vernon, W. H. J., Wormwell, F. and Nurse, T. J.: J. Chem. Soc., (1939), p. 621.
32) Rhodin, T. N.: Ann. N. Y. Acad. Sci., 58 (1954), p. 855.
33) Hoar, T. P., Talerman, M. and Sherwood, P. M. A.: Nature. Phys. Sci., 240 (1972), p. 116.
34) Bancroft, G. M., Mayne, J. E. O. and Ridgway, P.: Brit. Corros. J., 6 (1971), p. 119.
35) Wingrove, J.: J. Iron and Steel Inst., March (1970), p. 258.
36) Darken, L. S. and Gurry, R. W.: J. Amer. Chem. Soc., 67 (1945), p. 1398.
37) Schenck, R. and Dingmann, T.: Z. anorg. Chem., 166 (1927), p. 113.
38) Jette, E. R. and Foote, F.: Trans. AIME, 105 (1933), p. 276.
39) Pfeil, L. B.: JISI, 123 (1931), p. 237.
40) Hansen, M.: 'Constitution of binary alloys' (1958), p. 686., McGraw Hill Pub,
41) Bruce, D. and Hancock, P.: Br. Corros. J., 4 (1969), p. 221.
42) Bateman, G. J. and Rolls, R.: Br. Corros. J., 5 (1970), p. 122.
43) Cowan II, R. L. and Tedman Jr., C. S.: in 'Advanced Corrosion Science and Technology,' vol 3rd. (1974). Ed. by Mars G. Fontana and Roger W. Staehle, Plenum Press. N. Y.
44) Noden, J. D., Knights, C. J. and Thomas, M. W.: Br. Corros. J., 3 (1968), p. 47.
45) Brusic, V.: Oxide Films, 1 (1972), p. 1.
46) Hoar, T. P.: Corros. Sci., 7 (1967), p. 341.
47) Engel, H. J. and Stolica, N. D.: Z. Phys. Chem., 215 (1960), p. 167.
48) Hoar, T. P., Mears, D. C. and Rothwell, G. P.: Corros. Sci. 5 (1965), p. 279.
49) Hoar, T. P. and Mears, D. C.: Proc. Royal Soc. (London)., A 294 (1966), p. 486.
50) Breiter, M. W.: Electrochim. Acta., 15 (1970), p. 1195.
51) Nagayama, M. and Cohen, M.: J. Electrochem. Soc., 110 (1963), p. 670.
52) Nagayama, M. and Cohen, M.: J. Electrochem. Soc., 109 (1962), p. 781.
53) Novakovsky, V. M. and Likhachev, M. A.: Electrochim. Acta: 12, (1967), p. 267.
54) Wagner, C. and Traud, W.: Z. Elektrochem., 44 (1938), p. 391.
55) Mansfeld, F.: Corros. -NACE, 29 (1973) 10, p. 397.
56) Vijh, A. K.: J. Mater. Sci., 8 (1973), p. 1669.
57) Idem,: "Electrochemistry of Metals and Semiconductors," Marcel Dekker, New York (1973).
58) Vijh, A. K.: Corros. Sci., 11 (1971), p. 411.
59) Eremias, B. and Prazak, M.: Corros. Sci., 13 (1973), p. 907.
60) Epelboin, I. and Keddam, M. Electrochim. Acta., 17 (1972), p. 117.
61) Gilroy, D. and Conway, B. E.: J. Phys. Chem., 69 (1965), p. 1251.
62) De Levie, R. and Pospisil, L.: Electroanal. Chem., 22 (1969), p. 277.
63) Murgulescu, I. G. and Radovici, O.: Proc. 17th Meeting CITCE, Tokyo (1966).
64) Ebersbach, V., Schwabe, K. and Pitter, K.: Electrochim. Acta., 12 (1967), p. 927.
65) Losev, V. V. and Pcheelnikov, A. P.: Electrochim. Acta., 18 (1973), p. 589.